The log $k_{d,obsd}$ value increased linearly with pH. This cannot be explained by the increase in the neutral VIm unit because the VIm unit is almost completely dissociated in this pH range ($\alpha_{VIm} > 0.85$ above pH 7). When plotted against α_{VIm}, $k_{d,obsd}$ shows a steep rise as α_{VIm} approaches unity. A similar result was found previously for bifunctional polymer **8**.[4] Probably, the polymer molecule forms a tighter coil as the charge density decreases ($\alpha_{VIm} \rightarrow 1$), thus enhancing the catalytic efficiency of the intramolecular VIm group.

Substrate Binding. The hydrolysis of NNBA (**7**) by the MHA-VIm copolymer (**1**) proceeds according to the Michaelis-Menten kinetics. On the other hand, no substrate binding was observed for the other three substrates. Therefore, both coulombic and hydrophobic attractions are required for efficient binding. The VIm unit must make an important contribution to substrate binding, since the MHA-AAm catalyst (**2**) did not bind NNBA (**7**). The binding tendency as given by $1/K_m$ decreases with increasing pH, indicating the coulombic contribution of the protonated VIm unit to substrate binding. The apparent rate of the intracomplex catalysis, $k_{cal.}$, increases with increasing pH. This is attributed to the dissociation of the MHA unit. Detailed examination of the $k_{cal.}$ term cannot be done, though multiple acylation processes may be present. The apparent catalytic efficiency of the MHA-VIm copolymer, $k_{cal.}/K_m$, is greater by factors of 10–200 than that of the MHA-AAm copolymer (**2**) due to substrate binding.

Conclusion

In the charge relay system at the active site of serine proteases, the acylation and deacylation reactions at the seryl hydroxyl group are assisted by the general-base catalysis of the histidylimidazole group. Since the presence of the charge relay system was reported, considerable efforts have been directed to the preparation of model charge relay systems, with partial or little success. To our knowledge, the MHA-VIm copolymer (**1**) is the first hydrolytic catalyst in which both nucleophilic activation of the OH group and the accelerated hydrolysis of the acyl intermediate are made possible by the general-base assistance of the neighboring imidazole group. This catalytic scheme is very similar to that of the charge relay system in serine proteases,[6] except that the aspartic carboxylate anion is involved in the activation of the imidazole group in the enzyme system. The occurrence of substrate binding in the case of NNBA (**7**) renders the present system still more suitable as a proteolytic enzyme model. It is amazing that a simple vinyl copolymer such as MHA-VIm (**1**) can mimic several important characteristics of the serine protease action.

Acknowledgment. The authors appreciate the capable experimental assistance of Miss R. Ando. This investigation was supported by a grant-in-aid from the Ministry of Education.

References and Notes

(1) T. Kunitake and Y. Okahata, *Bioorg. Chem.*, **4**, 236–148 (1975).
(2) T. Kunitake and Y. Okahata, *Macromolecules*, **9**, 15 (1976).
(3) T. Kunitake and S. Horie, *Bull. Chem. Soc. Jpn.*, **48**, 1304–1309 (1975).
(4) T. Kunitake, Y. Okahata, and T. Tahara, *Bioorg. Chem.*, **5**, 155–167 (1976).
(5) Y. Kitaura and M. L. Bender, *Bioorg. Chem.*, **4**, 237–249 (1975).
(6) D. M. Blow, J. J. Birktoft, and B. S. Hartley, *Nature (London)*, **221**, 337–340 (1969).
(7) T. Maugh II and T. C. Bruice, *J. Am. Chem. Soc.*, **93**, 3237–3248 (1971).
(8) T. C. Bruice and I. Oka, *J. Am. Chem. Soc.*, **96**, 4500–4507 (1974).
(9) A. J. Kirby and G. J. Lloyd, *J. Chem. Soc., Perkin Trans. 2*, 637–642 (1974).
(10) T. Kunitake, F. Shimada, and C. Aso, *J. Am. Chem. Soc.*, **91**, 2716–2723 (1969).
(11) T. Kunitake, S. Shinkai, and S. Hirotsu, *J. Polym. Sci., Polym. Lett. Ed.*, **13**, 377–381 (1975).
(12) C. G. Overberger and I. Cho, *J. Polym. Sci., Polym. Chem. Ed.*, **6**, 2741–2754 (1968).
(13) J. H. Cooley, W. D. Bills, and J. R. Throckmorton, *J. Org. Chem.*, **25**, 1734–1736 (1960).
(14) A. Katchalsky, N. Shavit, and H. Eisenberg, *J. Polym. Sci.*, **13**, 69–84 (1954).
(15) R. Lumry, E. L. Smith, and R. R. Glantz, *J. Am. Chem. Soc.*, **73**, 4330–4340 (1951).
(16) M. L. Bender and T. H. Marshall, *J. Am. Chem. Soc.*, **90**, 201–207 (1968).
(17) T. Kunitake, Y. Okahata, and S. Hirotsu, *Bull. Chem. Soc. Jpn.*, in press.
(18) W. B. Gruhn and M. L. Bender, *Bioorg. Chem.*, **4**, 219–236 (1975).

Multifunctional Hydrolytic Catalyses. 8. Remarkable Acceleration of the Hydrolysis of *p*-Nitrophenyl Acetate by Micellar Bifunctional Catalysts[1]

Toyoki Kunitake,* Yoshio Okahata, and Tetsuo Sakamoto

Contribution No. 397 from the Department of Organic Synthesis, Faculty of Engineering, Kyushu University, Fukuoka 812, Japan. *Received March 16, 1976*

Abstract: Surfactant molecules which contain the hydroxamate and imidazole functions were synthesized, and their catalytic actions in aqueous cetyltrimethylammonium bromide micelles were examined for the hydrolysis of *p*-nitrophenyl acetate at 30 °C. The catalysis proceeded mainly via acylation and imidazole-catalyzed deacylation at the hydroxamate group. Both of these processes were remarkably accelerated in the case of bifunctional micelles, due to activation of anionic nucleophiles in cationic micellar environments. The overall catalytic efficiency exceeded even that of α-chymotrypsin at pH 8 and was more than 5000 times higher than that of imidazole. Micellar monofunctional catalysts and a nonmicellar bifunctional catalyst were much less effective. Therefore, the combination of bifunctionality and micellar microenvironments was essential for the highly efficient catalysis.

The high proteolytic activity of serine proteases is derived from fast acylation and deacylation at the seryl hydroxyl group. The remarkable efficiency of these processes is currently explained by the multifunctionality and the microenvironment of the catalytic site.[2]

In the previous papers of this series,[3,4] we have established that combinations of complementary functional groups such as hydroxamate and imidazole give rise to enhanced catalytic efficiency. However, the esterolytic efficiency of these bifunctional catalysts was still much lower than that of α-chymotrypsin.

The reactivity of anionic nucleophiles is remarkably enhanced in cationic micelles.[5] Therefore, it is expected that the efficiency of the bifunctional catalysts is further enhanced in

micellar microenvironments. We synthesized bifunctional surfactants and some reference compounds and examined their catalytic activities in the CTAB (cetyltrimethylammonium bromide) micelle toward the hydrolysis of *p*-nitrophenyl acetate.

LImHA (**1**) and LImPrHA (**4**) are bifunctional surfactants possessing hydroxamate and imidazole functions. LBHA (**6**), LImHA-Bz (**2**), and LImPrHA-Bz (**5**) are monofunctional surfactants possessing either one of the catalytic functions. MImHA (**3**) is a nonmicellar bifunctional compound.

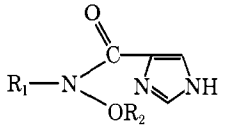

LImHA (**1**), $R_1 = CH_3-(CH_2)_{11}-$; $R_2 = H-$
LImHA-Bz (**2**), $R_1 = CH_3-(CH_2)_{11}-$; $R_2 = C_6H_5CH_2-$
MImHA (**3**), $R_1 = CH_3-$; $R_2 = H-$

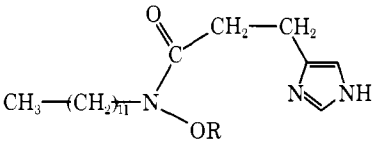

LImPrHA (**4**), R = H-
LImPrHA-Bz (**5**), R = $C_6H_5CH_2$-

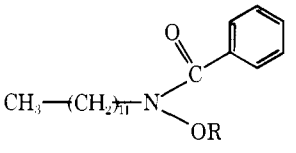

LBHA (**6**), R = H-
Ac-LBHA (**7**), R = $CH_3C(=O)$-

Experimental Section

Functional surfactants were prepared by the following routes. Spectroscopic (ir and NMR) data were consistent with the respective structures.

N-Laurylbenzohydroxamic Acid (LBHA, 6). Benzyl benzohydroxamate[4,7] (15.2 g, 0.07 mol) in dry DMF was added dropwise under nitrogen to 50% NaH (2.9 g, 0.06 mol) suspended in 300 ml of dry DMF. After 90% of the theoretical amount of hydrogen gas had evolved, a DMF solution of lauryl bromide (13.9 g, 0.05 mol) was added at once from a dropping funnel, and the mixture was stirred at 140–150 °C for 4 h. It was filtered and neutralized with dilute hydrochloric acid, and solvent was removed in vacuo to give 27 g of a pale yellow oil. The oil was dissolved in 100 ml of dry ethanol and hydrogenated for 2 h at the atmospheric pressure over 5% $Pd/SrCO_3$. The catalyst was removed by filtration, solvent was removed in vacuo, and the residual white solid was recrystallized twice from acetonitrile: mp 75–76 °C; yield 55%. Anal. ($C_{19}H_{35}O_2N$) C, H, N.

Acetyl *N*-Laurylbenzohydroxamate (Ac-LBHA, 7). Acetyl chloride (0.25 g, 0.033 mol) in 10 ml of dry ether was added dropwise to a stirred ethereal solution of 1.0 g (0.033 mol) of LBHA (**6**) and 0.33 g (0.033 mol) of triethylamine. Filtration and solvent removal gave colorless needles: yield 88%; mp 46–49 °C. Anal. ($C_{21}H_{33}NO_3$) C, H, N.

Benzyl *N*-Lauryl(4-imidazolecarbo)hydroxamate (LImHA-Bz, 2). Crude benzyl *N*-laurylbenzohydroxamate (10 g) was hydrolyzed in a mixture of 100 ml of ethanol and 30 ml of concentrated hydrochloric acid by refluxing for 6 h. Extraction with $CHCl_3$ and recrystallization from acetone, containing a drop of concentrated hydrochloric acid, gave *O*-benzyl-*N*-laurylhydroxylamine hydrochloride in 49% yield: mp 62–65 °C.

The hydrochloride (2.7 g, 0.009 mol) and 8.1 g (0.08 mol) of triethylamine in 10 ml of chloroform was added to 4-imidazolecarbonyl chloride hydrochloride[8] and heated to 60 °C for 4 h. 4-Imidazolecarboxylic acid was separated and the solvent removed to give LImHA-Bz (**2**) hydrochloride as a yellow solid. Recrystallizations from acetonitrile and chloroform gave colorless crystalline granules, mp 125–128 °C. Anal. ($C_{23}H_{36}N_3O_2Cl$) H, N; C: calcd, 65.48; found, 67.78.

***N*-Lauryl(4-imidazolecarbo)hydroxamic Acid (LImHA, 1).** The benzyl ester was hydrogenated over $Pd/SrCO_3$ and the white solid which formed was recrystallized from acetonitrile and ethanol: yield 40%; mp 181–184 °C dec. Anal. ($C_{16}H_{30}O_2N_2Cl$) C, H, N.

Benzyl *N*-Lauryl[β-(4-imidazole)propio]hydroxamate (LImPrHA-Bz, 5). β-(4-Imidazole)propionic acid hydrochloride, mp 125–127 °C,[9] was prepared by reduction (Zn-CH_3COOH) of α-chloro-β-imidazolepropionic acid and converted to its acid chloride with thionyl chloride and, without purification, allowed to react with

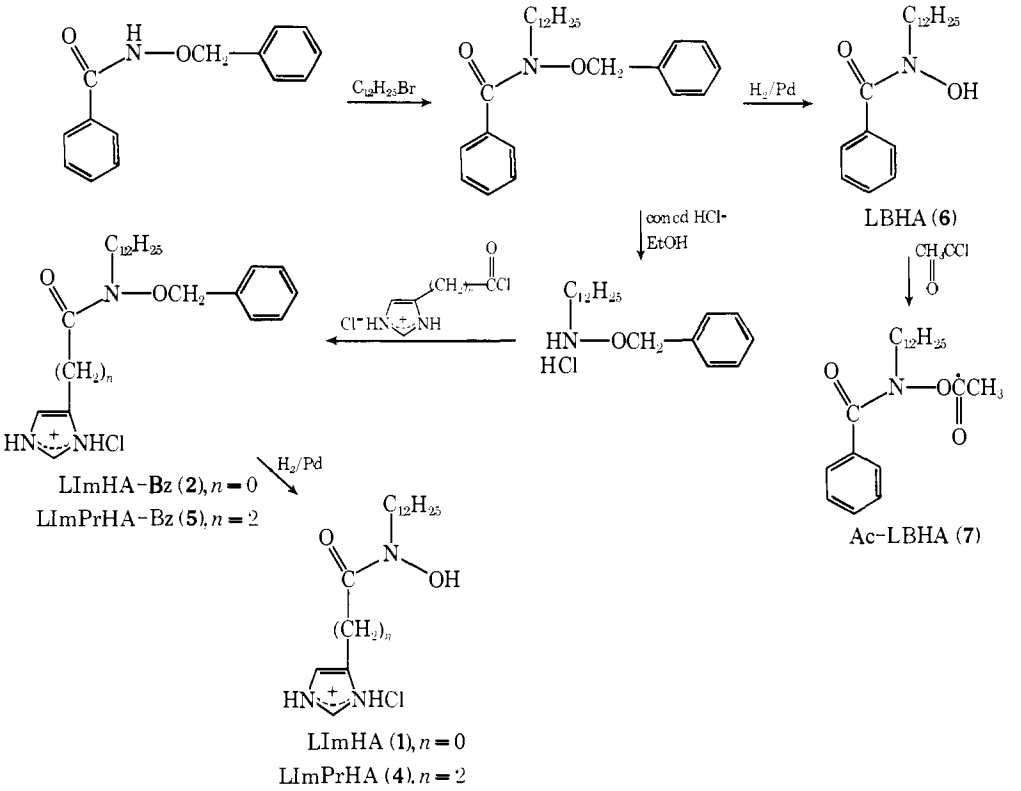

Table I. Dissociation Behavior of Hydroxamic Acid Groups in CTAB Micelles[a]

Catalyst	μ = 0.01 (KCl)		μ = 0.50 (KCl)	
	n'	pK_{app}	n'	pK_{app}
LImHA (**1**)	1.50	9.04	1.03	9.75
LImPrHA (**4**)	1.45	9.38	1.39	10.7
LBHA (**6**)	1.21	8.41	0.93	9.72

[a] 30 °C, 3 vol/vol % EtOH–H_2O, 3.38 × 10^{-3} M CTAB, 0.01 M borate buffer. Data are fitted to eq 2.

O-benzyl-*N*-laurylhydroxylamine hydrochloride. Recrystallizations from acetonitrile and ethanol gave colorless crystalline granules: yield 48%; mp 109–111 °C. Anal. ($C_{25}H_{40}O_2N_3Cl$) H, N; C: calcd, 66.72; found, 66.17.

***N*-Lauryl[*β*-(4-imidazole)propio]hydroxamic Acid (LImPrHA, 4).** The benzyl ester was hydrogenated in ethanol over Pd/$SrCO_3$. The resulting white powders were recrystallized from chloroform and acetonitrile: mp 80–83 °C; yield 35–45%. Anal. ($C_{18}H_{34}O_2N_3Cl$) H, N; C: calcd, 60.06; found, 59.32.

Other Materials. *N*-Methyl(4-imidazolecarbo)hydroxamic acid (MImHA, **3**) was reported previously.[6] *p*-Nitrophenyl acetate was recrystallized from cyclohexane, mp 78 °C. Commercial cetyltrimethylammonium bromide (CTAB) was recrystallized twice from water and the absence of impurities was confirmed by the measurement of the surface tension.[10]

Dissociation of Hydroxamic Acids. The degree of dissociation of hydroxamic acids, α_{HA}, was determined at 30 °C in 3 vol/vol % EtOH–H_2O in the presence of 3.38 × 10^{-3} M CTAB using the absorption coefficient at 300 nm [LImHA (**1**) and LBHA (**6**)] and at 250 nm (LImPrHA, **4**). The phototitration data could be fitted to the modified Henderson-Hasselbach equation (correlation coefficient >0.99)[11]

$$\mathrm{pH} = -n' \log \frac{\epsilon_{A^-} - \epsilon}{\epsilon - \epsilon_{HA}} + \mathrm{p}K_{app} \quad (1)$$

$$= -n' \log \frac{1 - \alpha_{HA}}{\alpha_{HA}} + \mathrm{p}K_{app} \quad (2)$$

where ϵ_{HA} and ϵ_{A^-} are the absorption coefficients of hydroxamic acids and their anions, respectively, and pK_{app} corresponds to the pH of half neutralization (α_{HA} = 0.5). The titration data are summarized in Table I.

Rate Measurements. The hydrolysis of *p*-nitrophenyl acetate (PNPA) was performed at 30 °C in 3 vol/vol % EtOH–H_2O, and the formation of the *p*-nitrophenolate anion was followed at 401 nm with a Hitachi 124 uv-visible spectrometer. The hydrolysis of Ac-LBHA (**7**) was followed by using the absorption of the hydroxamate anion at 300 nm (ϵ 1860). The kinetic constants were calculated by a programmable desk calculator (Sharp Co., Compet 364P) and the least-squares procedure was employed wherever possible. The correlation coefficient was better than 0.99 unless noted to the contrary.

Results

Kinetics. Examples of the hydrolysis of PNPA by several catalysts [LImHA (**1**), LImHA-Bz (**2**), LBHA (**6**), MImHA (**3**)] in the presence of CTAB are shown in Figure 1. The *p*-nitrophenol (P_l) release is much faster with the micellar bifunctional catalyst (LImHA, **1**) than with the nonmicellar bifunctional catalyst (MImHA, **3**). In particular, the efficiency of micellar LImHA (**1**) becomes very large at a low ionic strength (curve A'). *p*-Nitrophenol is produced in proportion to time in the case of the micellar imidazole catalyst (LImHA-Bz, **2**), and there is no accumulation of the acetyl intermediate. The reaction with LBHA (**6**) follows the pseudo-first-order kinetics without regeneration of LBHA (**6**). The *p*-nitrophenol release by LImHA (**1**) (and also by LImPrHA, **4**) occurs according to the typical burst kinetics: initial fast release followed by slower, steady release. The initial rate of hydrolysis in the presence of micellar LImHA (**1**) and

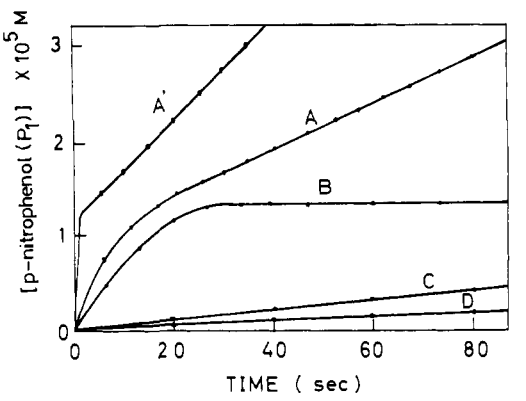

Figure 1. Time course of *p*-nitrophenol release: 30 °C, 3 vol/vol % EtOH–H_2O, μ = 0.5 (KCl), pH 8.80 (0.1 M Tris), [PNPA] = 1.05 × 10^{-4} M, [CTAB] = 1.03 × 10^{-3} M. A, [LImHA (**1**)] = 1.26 × 10^{-5} M; A', [LImHA (**1**)] = 1.32 × 10^{-5} M [μ = 0.01 (KCl), 0.01 M borate]; B, [LBHA (**6**)] = 1.26 × 10^{-5} M; C, [LImHA-Bz (**2**)] = 1.35 × 10^{-5} M; D, [MImHA (**4**)] = 1.35 × 10^{-5} M.

LImPrHA (**4**) was first order with PNPA up to at least 10^{-3} M. Therefore, substrate binding need not be considered.

The catalytic process is, thus, expressed by

$$C_{HA} + PNPA \xrightarrow{k_a} \underset{p\text{-nitrophenol}}{\overset{Ac\text{-}C_{HA}}{+}} \xrightarrow{k_d} C_{HA} + CH_3COOH \quad (3)$$

$$C_{Im} + PNPA \xrightarrow[slow]{k_{Im}} \underset{p\text{-nitrophenol}}{\overset{Ac\text{-}C_{Im}}{+}} \xrightarrow[fast]{} C_{Im} + CH_3COOH \quad (4)$$

where C_{HA} and C_{Im} denote hydroxamate and imidazole catalytic sites, respectively. The accumulation of the acetyl intermediate was not detected kinetically in the imidazole-catalyzed hydrolysis (eq 4).

The analysis of the burst kinetics has been successfully carried out with polymer catalysts.[3,12] However, it is necessary to confirm if the same kinetic analysis can be used in the micellar system.

The time course of the *p*-nitrophenol (P_l) release by the bifunctional catalyst is given by

$$[P_l] = A't + B(1 - e^{-bt}) \quad (5)$$

where

$$A' = \left[\frac{k_a \cdot k_d[PNPA]_0[C]_0}{k_a[PNPA]_0 + k_d}\right] + k_{Im}[PNPA]_0[C]_0$$

$$= k_d'[C]_0 \quad (6)$$

$$B = \frac{k_a^2[PNPA]_0^2[C]_0}{(k_a[PNPA]_0 + k_d)^2} \quad (7)$$

$$b = k_a[PNPA]_0 + k_d \quad (8)$$

and A', B, and b values are determined from the burst curve. The validity of this treatment in the micellar reaction was confirmed as follows.

In the LImHA (**1**)–CTAB system, the PNPA hydrolysis was studied with varying concentrations of catalyst (series I) and substrate (series II), and the experimental parameters (A', B, and b) were obtained as shown in Table II. In series I, A' and B values increased linearly with increasing LImHA (**1**) concentration, but the b value remained constant. These results are consistent with eq 6–8. In series II experiments, there is a linear relation between b and $[PNPA]_0$, and $k_{a,obsd}$ = 47.4

Table II. Burst Kinetics[a]

Series	10^5[LImHA (1)], M	10^4[PNPA], M	$10^8A'$, M s^{-1}	10^5B, M	10^2b, s^{-1}	$k_{a,obsd}$, M^{-1} s^{-1}	$k_{1m,obsd}$, M^{-1} s^{-1}	$10^3k_{d,obsd}$, s^{-1}
I	1.24	2.85	0.74	1.04	1.53	49.5	<1	1.24
	2.48	2.85	1.38	2.12	1.48	50.8	<1	1.07
	3.72	2.85	2.08	3.30	1.50	51.3	<1	0.98
II	2.48	1.90	1.04	2.01	1.08	51.4	<1	1.08
	2.48	2.37	1.23	2.18	1.29	51.1	<1	0.80
	2.48	2.85	1.48	2.22	1.53	49.4	<1	1.24

[a] 30 °C, 3 vol/vol % EtOH-H_2O, μ = 0.5 (KCl), 0.1 M Tris buffer, pH 7.43 ± 0.08, [CTAB] = 1.03 × 10^{-3} M.

Table III. Effect of Ionic Strength on Rate Constant[a]

Catalyst	Ionic strength (KCl)	α_{HA}	$k_{a,obsd}$, M^{-1} s^{-1}	$10^3k_{d,obsd}$, s^{-1}
LImHA (1)-CTAB	0.01[b]	0.48	2050[d]	390[e]
LImHA (1)-CTAB	0.50[c]	0.16	700	2.5
LImPrHA (4)-CTAB	0.01[b]	0.35	3050	4.0
LBHA (6)-CTAB	0.01[b]	0.75	1880	1.1
LBHA (6)-CTAB	0.50[c]	0.14	350	0.04

[a] 30 °C, pH 9.0 ± 0.1, 3 vol/vol % EtOH-H_2O, 1.02 × 10^{-3} M CTAB. [b] 0.01 M borate buffer. [c] 0.10 M Tris buffer. [d] $k'_{a,obsd}$ (eq 13). [e] $k'_{d,obsd}$ (eq 12).

M^{-1} s^{-1} and $k_{d,obsd}$ = 1.07 × 10^{-3} s^{-1} in accordance with eq 8.

The k_a and k_d values can be also determined from the presteady state by a single experiment.

$$k_a = \frac{b\sqrt{B}}{[PNPA]_0\sqrt{[C]_0}} \quad (9)$$

$$k_d = b - k_a[PNPA]_0 \quad (10)$$

The k_{1m} value is obtained from eq 6 by using k_a and k_d values calculated from eq 9 and 10. The kinetic constants thus determined are given in Table II.

The k_a and k_d values were further determined from the steady state data. The turnover rate of the hydroxamate group, A, is obtained from A' and k_{1m}.

$$A = \frac{k_a \cdot k_d \cdot [PNPA]_0[C]_0}{k_a[PNPA]_0 + k_d} = k_{1urnover}[C]_0 \quad (11)$$

The double reciprocal plot ($1/A$ vs. $1/[PNPA]_0$) using the data of Table II yielded $k_{a,obsd}$ = 48.8 M^{-1} s^{-1} and k_d = 1.22 × 10^{-3} s^{-1}.

The $k_{a,obsd}$ and $k_{d,obsd}$ values determined by three different methods (eq 8, eq 9 and 10, and eq 11) are very similar. This fact indicates that the burst experiments can be conducted with sufficient accuracy in the micellar system. The same conclusion was obtained with LImPrHA (4) catalyst.

The $k_{a,obsd}$ and $k_{d,obsd}$ values were preferentially determined from the analysis of the presteady kinetics (eq 9 and 10). In some cases, however, the initial burst was too rapid to be amenable to the kinetic analysis (cf. Figure 1, curve A'). Then, by putting $k_a[PNPA]_0 \gg k_d$, the following equation is derived from eq 6.

$$k_d' = k_d + k_{1m}[PNPA]_0 \quad (12)$$

The overall rate constant of the initial acylation, k_a', is separately determined under the pseudo-first-order condition ($[C]_0 \gg [PNPA]_0$).

$$k_a' = k_a + k_{1m} \quad (13)$$

As is discussed later, k_{1m} is negligibly small at pH <9, and k_a' and k_d' values are usually very close to k_a and k_d, respectively.

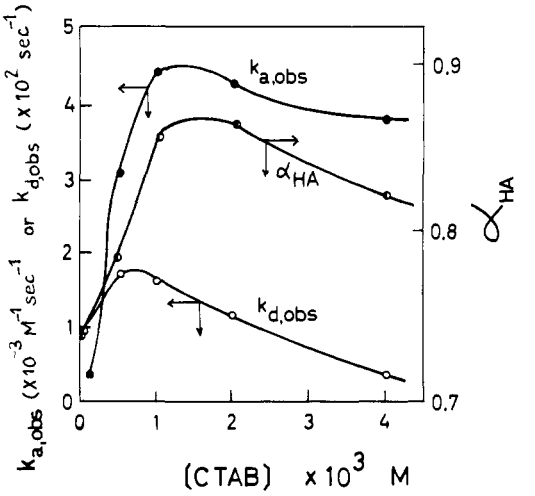

Figure 2. Effect of CTAB concentration on the rate constants at pH 9.3 and on α_{HA} at pH 10.4: 30 °C, 3 vol/vol % EtOH-H_2O, μ = 0.01 (KCl), 0.01 M borate buffer. [LImPrHA (4)] = 4.04 × 10^{-5} M.

The acylation rate with monofunctional catalysts [LBHA (6) and LImPrHA-Bz (5)] and the deacylation rate of Ac-LBHA (7) were determined under the pseudo-first-order condition.

Effect of Surfactant Concentration. The catalytic rate was sensitive to the CTAB concentration, and the rate-[CTAB] relation yielded bell-shaped profiles. For example, the variation of $k_{a,obsd}$ and $k_{d,obsd}$ values for LImPrHA (4) is shown in Figure 2. The maxima are observed at 1.0 × 10^{-3} M CTAB for $k_{a,obsd}$ and at 0.7 × 10^{-3} M for $k_{d,obsd}$. In the LImHA (1)-CTAB system, the rate maxima were similarly observed at [CTAB] = (0.5-1.0) × 10^{-3} M.

From measurements of the surface tension at 18 °C, the critical micelle concentration (cmc) was found to be 1.0 × 10^{-3} and 0.8 × 10^{-3} M in the absence and presence of the LImHA (1) catalyst (2 × 10^{-5} M), respectively. Thus, a small amount of the surfactant catalyst does not alter the micellar structure and those rate maxima that are obtained at the CTAB concentration near the cmc.

Also inserted in Figure 2 is the variation of α_{HA} of LImPrHA (4) at pH 10.4 with the CTAB concentration. The observed trend is very similar to that of $k_{a,obsd}$.

Effect of Ionic Strength. The micellar catalysis is usually inhibited with increased ionic strength.[10] This is the case with the present system, and both $k_{a,obsd}$ and $k_{d,obsd}$ rapidly decreased with increasing ionic strength. The rate constants at μ = 0.01 (KCl) and 0.5 (KCl) are compared in Table III. The $k_{a,obsd}$ and $k_{d,obsd}$ values are always larger at μ = 0.01. This variation is related to the change of α_{HA}. Thus, the ionic strength affects the rates by changing the dissociation behavior of the hydroxamate group (cf. Table I).

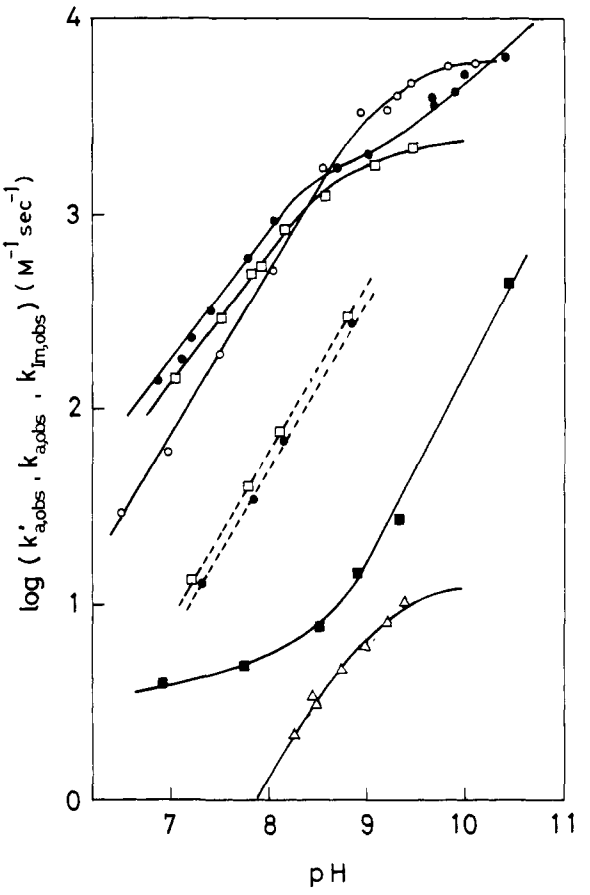

Figure 3. pH–rate profiles of acylation: 30 °C, 3 vol/vol % EtOH–H_2O; (—) μ = 0.01 (KCl), 0.01 M borate buffer; (- - -) μ = 0.5 (KCl), 0.1 M Tris buffer; (●) LImHA (**1**)-CTAB ($k'_{a,obsd}$); (○) LImPrHA (**4**)-CTAB ($k'_{a,obsd}$); (□) LBHA (**6**)-CTAB ($k_{a,obsd}$); (■) LImPrHA-Bz (**5**)-CTAB ($k_{Im,obsd}$); (△) MImHA (**3**) [$k_{a,obsd}$, 30 °C, 28.9 vol/vol % EtOH–H_2O, μ = 0.1 (KCl), 0.1 M Tris buffer].

pH–Rate Profiles of Acylation. Figure 3 shows pH–rate profiles of the acylation process. The $k_{a,obsd}$ and $k_{Im,obsd}$ values were determined from the burst kinetics and $k'_{a,obsd}$ (eq 13) is plotted for the LImPrHA (**4**)-CTAB system. In the case of LImHA (**1**), LBHA (**6**), and LImPrHA-Bz (**5**), $k'_{a,obsd}$, $k_{a,obsd}$, and $k_{Im,obsd}$ were obtained, respectively, from the pseudo-first-order kinetics. The increase in ionic strength from 0.01 to 0.5 resulted in rate decreases by a factor of ca. 10 over the pH range studied.

The $k_{Im,obsd}$ value of LImPrHA-Bz (**5**) is $1/50$–$1/100$ of $k'_{a,obsd}$ of LImPrHA (**4**). Therefore, the acylation reaction of the micellar bifunctional catalysts must occur predominantly at the hydroxamate site, i.e., $k_{a,obsd} \gg k_{Im,obsd}$. The micellar hydroxamates are ca. 1000 times more reactive than the nonmicellar hydroxamate (MImHA, **3**). The $k'_{a,obsd} - \alpha_{HA}$ plots are given in Figure 4. A line passing though the origin was obtained for the monofunctional LBHA (**6**), indicating that only the hydroxamate anion is effective for the acylation.

The bifunctional catalysts, LImHA (**1**) and LImPrHA (**4**), should possess the dissociation behavior illustrated in Scheme I. In the case of LImPrHA (**4**), the observed linear relation between $k'_{a,obsd}$ and α_{HA} indicates that the hydroxamate anion (monoanionic species in Scheme I) was the only effective nucleophile. The acylations at the undissociated hydroxamic acid and at the imidazole group are excluded.

On the other hand, the plots for LImHA (**1**) consisted of a linear portion at $\alpha_{HA} < 0.5$ and upward curvature at $\alpha_{HA} > 0.5$. Therefore, the dianionic species must become effective at the high pH region, in addition to the monoanionic species. The enhanced reactivity of the dianionic species relative to that of

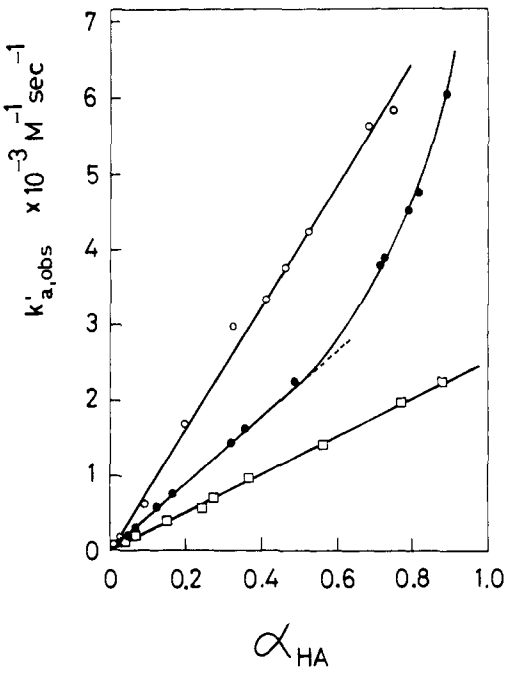

Figure 4. Dependence of rate constants of acylation ($k'_{a,obsd}$) on α_{HA}: 30 °C, 3 vol/vol % EtOH–H_2O, μ = 0.01 (KCl), 0.01 M borate buffer; (●) LImHA (**1**)-CTAB; (○) LImPrHA (**4**)-CTAB; (□) LBHA (**6**)-CTAB.

Scheme I

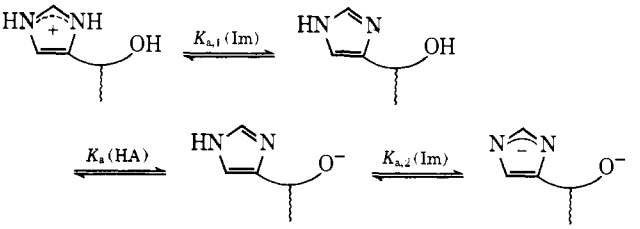

the monoanionic species may arise from (1) the increased reactivity of the hydroxamate anion and/or (2) the imidazole anion acting as a nucleophile. We have previously shown that the reactivity of the salicylohydroxamate anion toward PNPA is enhanced more than ten times when the *o*-hydroxyl group is dissociated.[13] On the other hand, the imidazole anion possesses a very high nucleophilicity in cationic micelles.[14-17] Therefore, both of these two possibilities are likely. Unfortunately, $pK_{a,2}$ (Im) could not be determined, and the rate constant for the dianionic species was not obtainable.

The linear relations (and its extrapolation to α = 1) of Figure 4 give the second-order rate constant for hydroxamate anions, k_a. The k_a values are collected in Table IV. The pK_{app} and k_a values of LImPrHA (**4**) at varying CTAB concentrations were estimated from α_{HA} at pH 9.3 by assuming n' = 1.45 (cf. Table I) in eq 2.

pH–Rate Profiles of Deacylation. Figure 5 shows pH–rate profiles for the deacylation process. The efficiency of deacylation at pH 7–10 was in the order of LImHA (**1**) > LImPrHA (**4**) > LBHA (**6**). The linear relations of unit slope between log $k_{d,obsd}$ and pH suggest that the anionic species is responsible for deacylation.

The hydrolysis of Ac-LBHA(**7**) is simply hydroxide catalyzed. The $k_{d,obsd}$ value at μ = 0.5 (4.0×10^{-5} s^{-1}; 30 °C; 3 vol/vol % EtOH–H_2O; pH 9.0) is comparable to that of nonmicellar acetyl *N*-benzylbenzohydroxamate (7.8×10^{-5} s^{-1}; 30 °C; 28.9 vol/vol % EtOH–H_2O; pH 9.4).[4] The micellar effect is clearly noticed at μ = 0.01: $k_{d,obsd} = 1.0 \times 10^{-3}$ s^{-1} at pH 9.0.

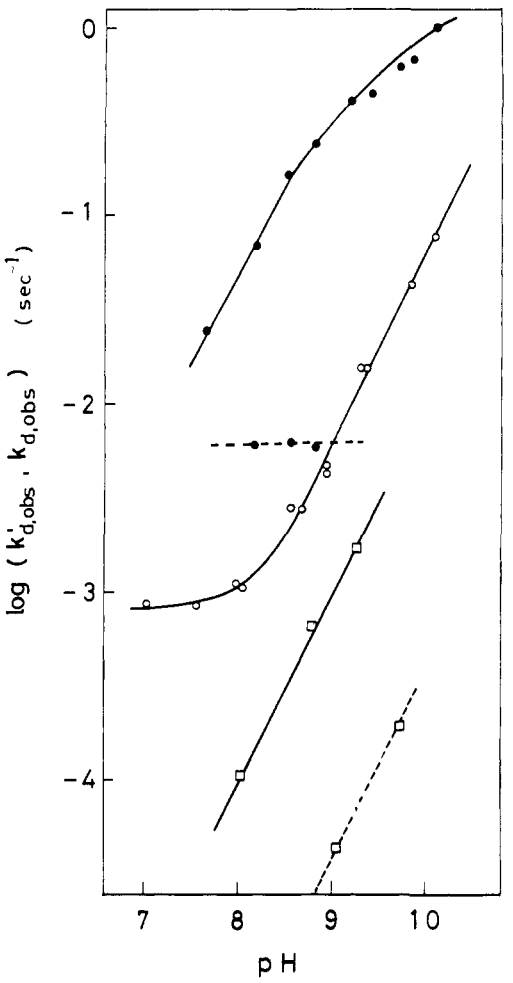

Figure 5. pH–rate profiles of deacylation: 30 °C, 3 vol/vol % EtOH–H_2O; (—) μ = 0.01 (KCl), 0.01 M borate buffer; (- - -) μ = 0.5 (KCl), 0.1 M Tris buffer. The plots for Ac-LBHA (**7**) were obtained by extrapolation to the zero buffer concentration: (●) LImHA (**1**)-CTAB ($k'_{d,obsd}$ for μ = 0.01 and $k_{d,obsd}$ for μ = 0.5); (○) LImPrHA (**4**)-CTAB ($k_{d,obsd}$); (□) Ac-LBHA (**7**)-CTAB ($k_{d,obsd}$).

In the case of bifunctional catalysts, the linear relation is explained by the involvement of the imidazole anion or its equivalent kinetic species. The $pK_{a,2}$ value for the imidazole group in *N*-lauryl(4-imidazolecarbo)amide was determined to be 10.45 in the presence of 1.03×10^{-3} M CTAB from the absorption of the imidazole anion at 260 nm [ϵ 8930; 30 °C; μ = 0.01 (KCl); 3 vol/vol % EtOH–H_2O].[18] The imidazole group of the Ac-LImHA (**1**) intermediate is expected to have a similar $pK_{a,2}$ value. The reactivity of the imidazole anion toward PNPA is appreciably enhanced in the CTAB micelle, whereas that of the neutral imidazole is suppressed.[17] Therefore, contribution of the anionic imidazole to the deacylation process may be significant even at lower pH. The $pK_{a,2}$ values for Ac-LImPrHA (**4**) will be higher by ca. 2 pH units than that for acetyl LImHA (**1**), because the imidazole group is not conjugated with the carbonyl group in the former compound. As a result, the linear relation of unit slope shifts to the higher pH region for Ac-LImPrHA (**4**), and the pH-independent portion appears in the low pH region where deacylation proceeds only through catalysis of the neutral imidazole species. The $pK_{a,2}$ (Im) value of Ac-LImHA (**1**) must become higher by increasing ionic strength from 0.01 to 0.5, and the neutral imidazole species becomes predominantly involved in deacylation, as inferred from the pH-independent $k_{d,obsd}$ values at μ = 0.5.

The k_d' value (eq 12) was adopted instead of $k_{d,obsd}$ for LImHA (**1**) (μ = 0.01), because the latter rate constant could not be determined due to too rapid initial burst. The contribution of the k_{Im} term to k_d' will not be significant at pH <9 where the anionic imidazole species is little formed.

Table IV. Acidity and Rate Constants of Acylation of Hydroxamates[a]

No.	Catalyst	10^3[CTAB], M	Ionic strength (KCl)	pK_{app}	k_a, $M^{-1}s^{-1}$
1	LImHA (**1**)	1.03	0.01	9.04	4380
2	LImHA (**1**)	1.03	0.50[b]	9.75	7720
3	LImPrHA (**4**)	0	0.01	9.95	30
4	LImPrHA (**4**)	0.50	0.01	9.55	6860
5	LImPrHA (**4**)	1.03	0.01	9.38	8160
6	LImPrHA (**4**)	1.03	0.50	10.7	6210
7	LImPrHA (**4**)	2.06	0.01	9.32	7610
8	LImPrHA (**4**)	3.10	0.01	9.41	8020
9	LBHA (**6**)	1.03	0.01	8.41	2560
10	LBHA (**6**)	1.03	0.50[b]	9.72	3090

[a] 30 °C, 3 vol/vol % EtOH–H_2O, 0.01 M borate buffer. [b] 0.1 M Tris buffer.

Table V. Catalytic Efficiency (pH 8.0 ± 0.2, [PNPA] = 1×10^{-4} M)

Catalyst	$k_{a,obsd}$, $M^{-1}s^{-1}$	$10^4 k_{d,obsd}$, s^{-1}	$10^4 k_{turnover}$, s^{-1}
LImHA (**1**)-CTAB[a]	930	650	380
LImPrHA (**4**)-CTAB[a]	510	9.6	9.4
LBHA (**6**)-CTAB[a]	490	0.13	0.13
MImHA (**3**)[b]	1.9	4	1.3
Imidazole[b]	0.07	0.33	0.07
α-Chymotrypsin[c]	400[d]	250	150

[a] 30 °C, 3 vol/vol % EtOH–H_2O, μ = 0.01 (KCl), 0.01 M borate buffer. [b] 30 °C, 28.9 vol/vol % EtOH–H_2O, μ = 0.1 (KCl), 0.1 M Tris buffer. [c] Reference 19; 25 °C, 20 vol/vol % isopropyl alcohol–H_2O. [d] $k_{a,obsd} = k_{cat.}/(K_m + [PNPA])$, $K_m = 7.7 \times 10^{-3}$ M, $k_{cat.}$ = 3.15 s^{-1}.

Discussion

Catalytic Efficiency. The catalytic cycle of the bifunctional micelles is given by Scheme II. The predominant course of

Scheme II

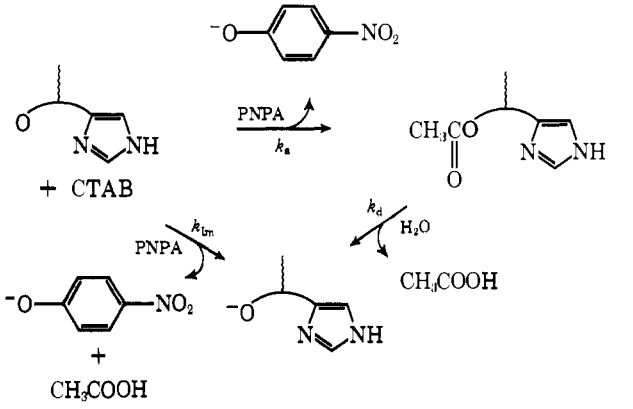

catalysis is the acyl transfer to the hydroxamate anion and the subsequent hydrolysis of the acyl intermediate by the intramolecular imidazole catalysis. The concerted acylation mechanism as reported in the accompanying paper[12] is not operating. The detailed mechanism of the imidazole catalysis

in deacylation (nucleophilic, general base, etc.) could not be elucidated, because the solvent isotope effect is not reliable in the micellar system. However, the major aim of this study is fulfilled, since both of the acylation and deacylation processes are remarkably accelerated.

The catalytic efficiency is most appropriately evaluated by $k_{1urnover}$ of eq 11. In Table V are compared the $k_{1urnover}$ value of several catalytic systems at pH 8, [PNPA] = 1×10^{-4} M. It is worth emphasizing that the LImHA (**1**)-CTAB system gives a $k_{1urnover}$ value which is more than two times larger than that of α-chymotrypsin. The catalytic efficiency of α-chymotrypsin is optimal at pH ~8 and $k_{a,obsd}$ tends to saturate at higher substrate concentrations ($K_m = 7.7 \times 10^{-3}$ M).[19] On the other hand, the LImHA (**1**)-CTAB system will have higher efficiencies by increasing pH of the medium and the substrate concentration. Thus, $k_{1urnover} = 1.33 \times 10^{-1}$ s^{-1} at pH 9, [PNPA] = 1×10^{-4} M, a value at least eight times greater than that of α-chymotrypsin. The other micellar bifunctional catalyst, LImPrHA (**4**)-CTAB, is much less efficient at pH 8 because of low $k_{d,obsd}$. This is attributed to the lower p$K_{a,2}$ value of the nonconjugated imidazole group. The micellar monofunctional catalyst, LBHA (**6**)-CTAB, is much less efficient, because $k_{d,obsd}$ is very small in the absence of the intramolecular imidazole group. On the other hand, the low efficiency of the nonmicellar bifunctional system, MImHA (**3**), is ascribed to the low values of both of $k_{a,obsd}$ and $k_{d,obsd}$. The relative efficiency of the acylation and deacylation processes at [PNPA] = 10^{-4} M is given by directly comparing the figures of the second and third columns of Table V. It is clear that the high catalytic efficiency is attained by the optimum balance of the k_a and k_d values.

It would be useful to compare the catalytic efficiency observed in this study with those reported by other workers. There have been many investigations on the catalytic hydrolysis of PNPA by nucleophilic micelles and related systems.[20,21] Most of these investigations were conducted under the pseudo-first-order condition; i.e., only the acylation process was followed. The highest rate constants of acylation were reported for long-chain aliphatic hydroxamates in micellar[22] and polysoap[23] systems, which are comparable to the acylation rate presented herein. However, the catalytic efficiency of these monofunctional micelles is very small, because of slow deacylation (see above).

On the other hand, Martinek and others[24] hydrolyzed PNPA in octadecyldiethylhydroxyethylammonium bromide micelles and obtained the following rate constants: $k_{a,obsd}$ = 320 M^{-1} s^{-1} and $k_{d,obsd}$ = ~10^{-4} s^{-1} at 30 °C, pH 8.5. A bifunctional (alkoxyl and imidazole) micelle recently reported by Moss and others[21] showed only a limited nucleophilicity. Thus, the present bifunctional micelle is by far the best catalyst for the hydrolysis of phenyl esters.

Nature of the Micellar Catalysis. An interesting, recent development in the micellar catalysis is remarkable enhancements of the reactivity of some anionic nucleophiles in cationic micelles and in cationic polysoaps. We concluded that the large rate enhancement observed is mostly derived from formation of hydrophobic, desolvated ion pairs between anionic nucleophiles and cationic surfactant molecules.[5] The high charge density at the micellar surface does not seem to be a prerequisite for the rate enhancement. The formation of hydrophobic ion pairs would increase the rate by the increased amounts of anionic species due to pK_{app} lowering and by the increased reactivity of a given anionic nucleophile.

Figure 6 shows the log k_a − pK_{app} plot for micellar and nonmicellar hydroxamates. Two major conclusions may be drawn from Figure 6. One is that there exist rate differences of ca. 100 times between the micellar and nonmicellar catalysts, and this difference most probably arises from formation of hydroxamate ion pairs in hydrophobic environments of the micellar phase. In fact, tetraalkylammonium hydroxamates showed much higher reactivities in dry, aprotic solvents than in protic solvents.[25] The second conclusion is that k_a is not altered appreciably by variations of ionic strength and the CTAB concentration. In contrast, pK_{app} shifts are considerable (see Table IV). That is, the characteristics of the micellar surface, such as charge density, are readily affected by ionic strength and CTAB concentration, and hence, pK_{app} shifts of the catalytic group of bound surfactants. However, the hydroxamate ion pair, once formed in the hydrophobic region of the micellar phase, would have fairly constant reactivity. This conclusion is consistent with the concept of the hydrophobic ion pair.

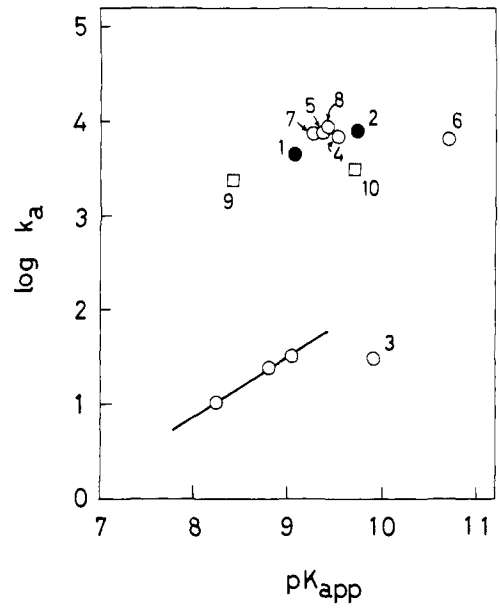

Figure 6. Bronsted plots for the reaction of hydroxamates with PNPA: 30 °C, 3 vol/vol % EtOH-H_2O. The numbers indicate those recorded in Table IV. The relation given by solid line was obtained for the reaction of simple, nonmicellar hydroxamates with PNPA [ref 5, 30 °C, 1.4 vol/vol % CH_3CN-H_2O, μ = 0.1 (KCl)].

Concluding Remark. The micellar, bifunctional systems can act as very powerful hydrolytic catalysts. In particular, the LImHA (**1**)-CTAB system possessed a catalytic efficiency surpassing that of α-chymotrypsin at pH 8, though for a nonspecific substrate. The activity difference would become greater at a higher pH of the medium. In terms of $k_{1urnover}$, this catalytic efficiency is more than 5000 times larger than that of imidazole, the first model of hydrolytic enzymes.

This remarkable rate acceleration was brought forth by the presence of complementary catalytic groups in the micellar environment.

References and Notes

(1) For a preliminary report of this study, see T. Kunitake, Y. Okahata, and T. Sakamoto, *Chem. Lett.*, 459–462 (1975).
(2) See, for example, P. D. Boyer Ed., "The Enzymes", Vol. 3, Academic Press, New York, N.Y., 1971, pp 165–353.
(3) T. Kunitake and Y. Okahata, *Macromolecules*, **9**, 15 (1976).
(4) T. Kunitake, Y. Okahata, and T. Tahara, *Bioorg. Chem.*, **5**, 155–167 (1976).
(5) *E.g.*, T. Kunitake, S. Shinkai, and Y. Okahata, *Bull. Chem. Soc. Jpn.*, **49**, 540–545 (1976).
(6) T. Kunitake and S. Horie, *Bull. Chem. Soc. Jpn.*, **48**, 1304–1309 (1975).
(7) J. H. Cooley, W. D. Bills, and J. R. Throckmorton, *J. Org. Chem.*, **25**, 1734–1736 (1960).
(8) This compound was prepared from 2.0 g (0.0089 mol) of 4-imidazolecarboxylic acid and 3.4 g of PCl_5 and used without purification.[6]
(9) S. Frankel, *Beitr. Chem. Physiol. Pathol.*, **8**, 156–162 (1906).
(10) J. H. Fendler and E. J. Fendler, "Catalysis in Micellar and Macromolecular Systems", Academic Press, New York, N.Y., 1975, Chapter 1.
(11) A. Katchalsky, N. Shavit, and H. Eisenberg, *J. Polym. Sci.*, **13**, 69–84 (1954).

(12) T. Kunitake and Y. Okahata, *J. Am. Chem. Soc.*, preceding paper in this issue.
(13) T. Kunitake, Y. Okahata, and S. Hirotsu, *Bull. Chem. Soc. Jpn.*, in press.
(14) W. Tagaki, M. Chigira, T. Amada, and Y. Yano, *Chem. Commun.*, 219–220 (1972).
(15) P. Heitmann, R. Husung-Bubtitz, and H. J. Zunft, *Tetrahedron*, **30**, 4137–4140 (1974).
(16) K. Martinek, A. P. Osipov, A. K. Yatsimirski, V. A. Dadali, and I. V. Berezin, *Tetrahedron Lett.*, 1279–1282 (1975).
(17) K. Martinek, A. P. Osipov, A. K. Yatsimirski, and I. V. Berezin, *Tetrahedron*, **31**, 709–718 (1975).
(18) Y. Okahata, unpublished results in these laboratories.
(19) H. Gutfreund and J. M. Sturtevant, *Biochem. J.*, **63**, 656–661 (1956).
(20) See ref 10, Chapter 5, pp 169–189.
(21) R. A. Moss, R. C. Nahas, S. Ramaswami, and W. J. Sanders, *Tetrahedron Lett.*, 3379–3382 (1975).
(22) I. Tabushi, Y. Kuroda, and S. Kita, *Tetrahedron Lett.*, 643–646 (1974).
(23) T. Kunitake, S. Shinkai, and S. Hirotsu, *J. Polym. Sci, Polym. Lett. Ed.*, **13**, 377–381 (1975).
(24) K. Martinek, A. V. Levashov, and I. V. Berezin, *Tetrahedron Lett.*, 1275–1278 (1975).
(25) S. Shinkai and T. Kunitake, *Chem. Lett.*, 109–112 (1976).

Calculations of Optical Properties of Biliverdin in Various Conformations

G. Wagnière and G. Blauer*

Contribution from the Institute of Physical Chemistry, University of Zurich, 8001 Zurich, Switzerland, and Department of Biological Chemistry, The Hebrew University, Jerusalem, Israel. *Received April 15, 1976*

Abstract: Experimentally observed longer wavelength light-absorption and CD spectra of biliverdin–serum albumin complexes were compared with spectra calculated by an SCF-MO-CI procedure in the frame of an adapted PPP approximation and of the CNDO approximation. A number of selected bile-pigment conformations produced by skewing of bonds at the methene bridges were considered. Both initially "open" and "ring-like" structures of the biliverdin skeleton were taken into account. The variation of spectral changes with conformation indicates improved agreement between theory and experiment in certain intermediate forms between "open" and "ring-like" conformations rather than at either of the extremes. Such intermediate conformations can be produced by skewing a bond at an "outer" methene bridge, in addition to skewing it at the "inner" bridge. The present data give additional weight to the concept that the light absorption of bile pigments and related chromophores, such as those of phytochrome and phycocyanins, depends markedly on their molecular geometry.

In a previously reported work[1] we have tried to compute the absorption and CD spectra of the physiologically important tetrapyrrole bile pigments, bilirubin and biliverdin. The experimentally determined optical properties of the highly specific 1:1 complexes of these bile pigments with serum albumin in aqueous solution[2-5] were compared with those calculated by a suitable SCF-MO-CI procedure using the PPP approximation.[6] Local σ-π separation was assumed in the dipyrromethene chromophores.[1] In order to simplify these calculations, the side chains of both bilirubin and biliverdin were ignored. In the case of bilirubin, the observed energy splitting between the two longest wavelength transitions as well as the sign and magnitude of the corresponding rotatory strengths observed under various conditions was correlated semiquantitatively with the data calculated for various conformations of the bile pigment. These conformations were obtained by changing the magnitude and the sign of the two dihedral angles of rotation around the two single carbon–carbon bonds separating the two dipyrromethenes of bilirubin. An analogous treatment of the biliverdin skeleton at the center methene bridge did not result in satisfactory agreement between experimental and calculated absorption or CD spectra, except for the appearance of the longest wavelength band on the red edge of the spectrum. The latter would be expected for this highly conjugated system in which a methene bridge connects the two dipyrromethene chromophores. Thus, in contrast to bound bilirubin, the two longest wavelength transitions of biliverdin are widely separated and cannot be interpreted in terms of a splitting of the exciton type. The conformations of bound biliverdin considered were produced by skewing the center methene bonds of either "open" or "ring-like" structures. Since the ratio of the oscillator strengths of the two main observed transitions (near 660 and 380–390 nm, respectively) was intermediate between those of the "open" and "ring-like" conformations, it was suggested that some intermediate conformation of biliverdin or a mixture of "open" and "ring-like" structures were present in the material investigated.[1] Such intermediate conformations suggested for bound biliverdin, which should also be energetically reasonable, can be obtained by specific skewing of the chromophores around the dihedral angles assigned in pairs to *all three* methene bridges, while still assuming the individual five-membered rings to remain planar. This procedure is followed in the present work. It can be started from different planar structures and, obviously, it should involve a very large number of conformations. Even with fair agreement between theory and experiment, no selected conformation should be considered to be unique. The cases treated presently allow some limited conclusions on possible conformations of biliverdin.

Computations and Results. The dihedral angles δ_1–δ_6 which characterize the conformations of biliverdin are defined as a twist around the bonds of the methene bridges and are illustrated in Figure 1. The completely planar and closed conformation, which is sterically unlikely, has the values $\delta_1/\delta_2/\delta_3/\delta_4/\delta_5/\delta_6 = 0/0/0/0/0/0$. The sense of rotation for a given angle is determined by looking at the molecule from the corresponding end group toward the central carbon atom C-25. Counterclockwise rotation around a given bond i always corresponds to a positive increase of δ_i. If the nitrogen atoms are taken as pairwise equivalent, then the conformation 0/0/0/0/0/0 shows C_{2v} symmetry. All conformations for which simultaneously $\delta_1 = \delta_2$, $\delta_3 = \delta_4$, $\delta_5 = \delta_6$ then have a twofold axis of symmetry C_2, whereas in all cases with $\delta_1 = -\delta_2$, $\delta_3 = -\delta_4$, $\delta_5 = -\delta_6$ we find a plane of symmetry C_s.

In the choice of conformations to be considered in this investigation both nearly "ring-like" structures and very "open" geometries with δ_1 and δ_2 near 180° were ruled out for the reasons already indicated.[1] Furthermore, deviations of the